Dynamics of phonons in $Sr_3Ir_4Sn_{13}$: an experimental study by ultrafast spectroscopy measurements

2016 New J. Phys. 18 073045

(http://iopscience.iop.org/1367-2630/18/7/073045)

New Journal of Physics
The open access journal at the forefront of physics

Deutsche Physikalische Gesellschaft DPG
IOP Institute of Physics

Published in partnership with: Deutsche Physikalische Gesellschaft and the Institute of Physics

OPEN ACCESS

RECEIVED
12 April 2016

REVISED
15 June 2016

ACCEPTED FOR PUBLICATION
8 July 2016

PUBLISHED
26 July 2016

PAPER

Dynamics of phonons in $Sr_3Ir_4Sn_{13}$: an experimental study by ultrafast spectroscopy measurements

C W Luo[1,2], P C Cheng[1], C M Tu[1], C N Kuo[3], C M Wang[3] and C S Lue[2,3]

[1] Department of Electrophysics, National Chiao Tung University, Hsinchu 30010, Taiwan
[2] Taiwan Consortium of Emergent Crystalline Materials, Ministry of Science and Technology, Taipei 10601, Taiwan
[3] Department of Physics, National Cheng Kung University, Tainan 70101, Taiwan

E-mail: cwluo@g2.nctu.edu.tw **and** cslue@mail.ncku.edu.tw

Keywords: $Sr_3Ir_4Sn_{13}$, phonon, time resolved optical spectroscopy

Abstract

We report a study of ultrafast dynamics of photoexcited electrons and phonons in $Sr_3Ir_4Sn_{13}$ using dual-color transient reflectivity change ($\Delta R/R$) measurements. Time resolved optical spectroscopy of collective excitations reveal the marked features near its structural phase transition temperature $T^* \simeq 147$ K. Two distinctive oscillatory timescales in $\Delta R/R$ have been clearly resolved. The rapid THz-range oscillations are attributed to the dynamics of the optical phonons which strongly correlate to the structural phase transition. The slow GHz-range oscillatory phenomenon which only occurs below about 150 K is associated with the dynamic response of the longitudinal-acoustic phonons. These low-energy phonons show a softening feature on approaching the transition temperature, also indicating a strong relevance to the structural phase transition. The information that we demonstrated would provide a deeper understanding of the structural phase transition in $Sr_3Ir_4Sn_{13}$.

1. Introduction

The phase transition at $T^* \simeq 147$ K in $Sr_3Ir_4Sn_{13}$ has attracted attention due to indications of strong interplays with its superconductivity [1–6]. Single crystal x-ray diffraction (XRD) analysis for this material has confirmed the presence of a structural phase transition which has been identified as a lattice distortion from a high$-T$ cubic phase to a low$-T$ phase with lower crystallographic symmetry [1]. Further studies revealed that the phase transition at T^* is associated with a substantial reduction in the Fermi-level density of states (DOS) and has no involvement in any magnetic ordering. It has thus been speculated that the lattice distortion in $Sr_3Ir_4Sn_{13}$ could arise from the charge-density-wave (CDW) instability [1–4]. Moreover, a systematic suppression in T^* along with an enhancement in the superconducting transition temperature T_c has been established by introducing the hydrostatic and chemical pressure in $Sr_3Ir_4Sn_{13}$ [1]. This phenomenon bears a resemblance to those observed in the iron-pnictide superconducting systems such as $La(O_{1-x}F_x)FeAs$, $BaFe_2As_2$, and FeSe [7–10]. Unlike the cases of the iron-pnictide superconductors where the existence of the spin-density wave (SDW) state below T^* has become unambiguous [10–14], the scenario for the formation of the CDW state in $Sr_3Ir_4Sn_{13}$ has not been supported by direct experimental evidence.

In this work, we have carried out time-resolved ultrafast spectroscopy measurements on $Sr_3Ir_4Sn_{13}$ to obtain additional insight into the role of phonons in this material, essentially in connection with the observed anomalies at T^*. The ultrafast dynamics of $Sr_3Ir_4Sn_{13}$ was studied by measuring the photoinduced transient reflectivity changes ($\Delta R/R$) of the probe beam. Due to different time response for the photoinduced charge and lattice dynamics, it allows us to distinguish the role of the observed collective excitations in real time and to provide important information towards a deeper realization of the phase transition in $Sr_3Ir_4Sn_{13}$.

2. Experimental results and discussion

Single crystals of $Sr_3Ir_4Sn_{13}$ were grown by the tin self-flux method as described elsewhere [1, 3, 15]. A photograph of the growing crystal with dimensions of several millimeters is shown in the inset of figure 1(b). The

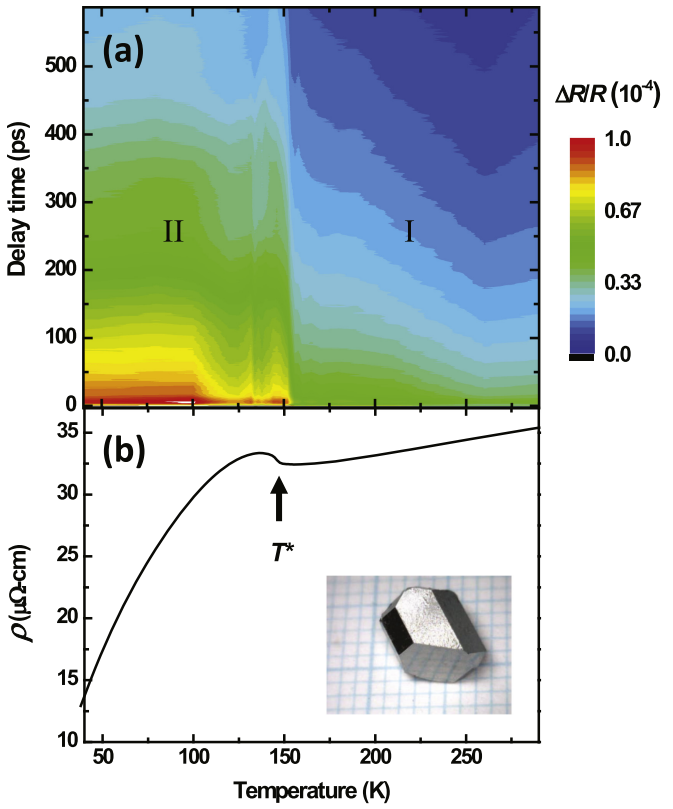

Figure 1. (a) Temperature and delay time variations of $\Delta R/R$ for $Sr_3Ir_4Sn_{13}$. (b) Temperature dependence of the electrical resistivity between 40 and 290 K. The arrow indicates the structural phase transition at T^*. Inset: photograph of the $Sr_3Ir_4Sn_{13}$ single crystal used in this study.

femtosecond (fs) spectroscopy measurements were performed using a dual-color pump-probe system (for the light source, the repetition rate: 5.2 MHz, the wavelength: 800 nm, the pulse duration: 100 fs) and an avalanche photo-detector with the standard lock-in technique. The pump beam is focused on the sample with a spot of about 92 μm in diameter; meanwhile, the spot of probe beam is 62 μm in diameter. The typical fluences of the pump beam and the probe beam are 61 (which was kept in the linear response region of pump-probe measurements) and 4.6 $\mu J\ cm^{-2}$, respectively. The pump pulses have the corresponding photon energy of 3.1 eV where the higher absorption occurs in $Sr_3Ir_4Sn_{13}$ and hence can generate electronic excitations. Here, the ultrafast dynamics of $Sr_3Ir_4Sn_{13}$ has been established by analyzing the data of $\Delta R/R$ of the probe beam with the photon energy of 1.55 eV.

Temperature and delay time variations of $\Delta R/R$ for $Sr_3Ir_4Sn_{13}$ are shown in figure 1(a). Two distinctive domains divided by T^* has been discerned. The dramatic change in $\Delta R/R$ across T^* is consistent with the hump feature in the electrical resistivity in the vicinity of T^*, as displayed in figure 1(b). To have a clear view for the entire response, we provide two typically temporal evolutions of $\Delta R/R$ measured at 40 K and 290 K in figure 2(a). It is noticeable that a slow oscillatory feature in $\Delta R/R$ was found at 40 K but no such phenomenon was observed at 290 K. An illustrative example demonstrating the oscillatory behavior at 40 K is given in the inset of figure 2(a). Detailed discussions about this observation will be described later.

Figure 2(b) shows two temporal evolutions of $\Delta R/R$ measured at 40 K and 290 K within several picoseconds (ps). For each temperature, a rapid and positive response together with a THz-range oscillation has been resolved. In the inset of figure 2(b), we provide a representative plot showing a fast oscillation at 40 K. The frequency of the oscillation corresponds to the energy of the emitted optical phonons. Unlike the slow oscillations, the phenomenon of the fast oscillation in $\Delta R/R$ appears in the entire temperature range we measured. To gain more insight on the evolution of $\Delta R/R$ across T^*, a three dimensional (3D) plot of $\Delta R/R$ as functions of temperature and delay time is displayed in figure 3.

In general, electronic excitations induced by a pump pulse would result in a swift rise in $\Delta R/R$ at zero delay time as observed. Since 5*d* electrons of Ir are dominant around the Fermi-level of $Sr_3Ir_4Sn_{13}$ [2], the observed excitation is mainly triggered by transferring the electrons from *d* valence band to the conduction band as schematically illustrated in the inset of figure 3. At zero delay time, the number of the photoexcited electrons generated by this non-thermal process is related to the amplitude of $\Delta R/R$. These high-energy electrons

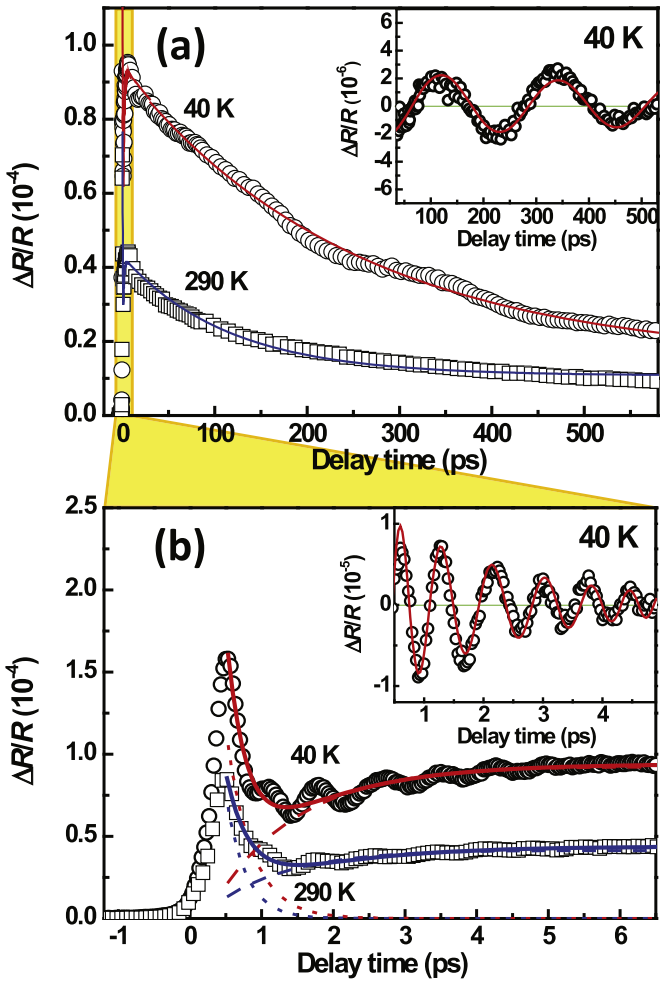

Figure 2. (a) The plots of $\Delta R/R$ versus decay time for 40 K and 290 K, respectively. Each solid curve represents the fitting result by employing equation (1). Inset: the slow oscillation signal obtained by subtracting the decay background at 40 K. The associated solid curve is the damped sinusoidal fitting. (b) An enlarged timescale of $\Delta R/R$ at 40 K and 290 K, respectively. The dotted and dashed lines represent the first and second terms of equation (1), as described in the text. The inset shows a fast oscillatory phenomenon with a damped sinusoidal fitting taken at 40 K.

accumulated in the *d* conduction bands quickly release their energy through the emission of optical phonons within several picoseconds. The optical phonons further decay via transferring energy to other phonon modes. In accordance with these processes, the decay background in $\Delta R/R$ can be phenomenologically described by

$$\frac{\Delta R}{R} = A_e e^{-t/\tau_e} + A_p(1 - e^{-t/\tau_r})e^{-t/\tau_p} + A_0 \quad (1)$$

The first term at the right-hand side of equation (1) is due to the decay of the excited electrons. Their initial population is related to the amplitude A_e and their relaxation process is characterized by the decay time τ_e. The second term describes the dynamics of the phonons related by an initial number A_p, a corresponding rise time τ_r, and a decay time τ_p . The last term A_o arises from the energy loss from the hot spot to the ambient environment within the timescale of microseconds, which is far longer than the period of our measurements (~575 ps) and hence is taken as a constant. With the employment of equation (1), the parameters in $\Delta R/R$ can be extracted for each temperature.

The extracted $T-$ dependent A_e and τ_e for $Sr_3Ir_4Sn_{13}$ are displayed in figure 4. For $T > T^*$, both A_e and τ_e exhibit weak temperature dependences, typical responses for an ordinary metal. With lowering temperature, A_e shows a rapid increase accompanied by a marked peak in the vicinity of T^*. The temperature variation of τ_e also exhibits a large enhancement across T^*. Since the magnitude of A_e is proportional to the initial population of photoexcited electrons, the dramatic change in A_e implies that a substantial reconstruction of electronic structures takes place undergoing the structural phase transition. This is consistent with the nuclear magnetic resonance (NMR) measurement which revealed sizeable reductions in both Sn and Ir electronic states in $Sr_3Ir_4Sn_{13}$ below T^* [3]. It is worthwhile mentioning that a broad maximum in A_e has been found at around 100 K. Such an observation is very likely due to intriguing electronic correlations, e.g., change of effective mass

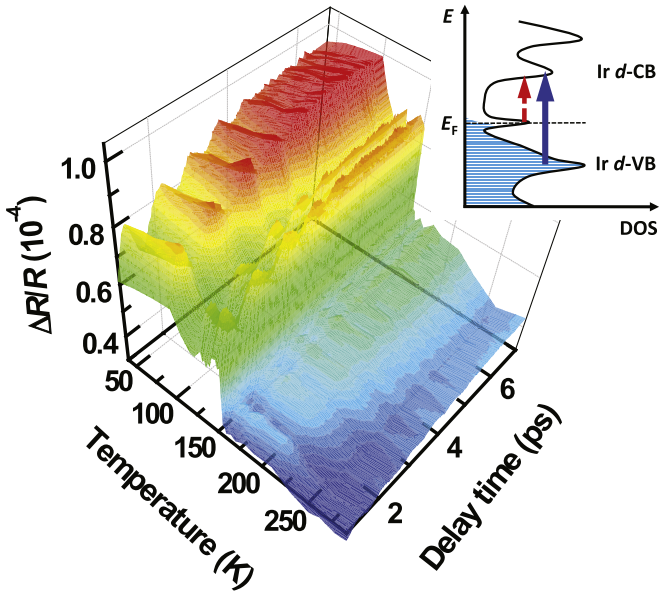

Figure 3. A 3D plot of $\Delta R/R$ with an enlarged timescale for $Sr_3Ir_4Sn_{13}$. The inset illustrates the schematically electronic band structure of $Sr_3Ir_4Sn_{13}$ and the pump-probe processes for 3.1-eV-pump (solid arrow) and 1.55-eV-probe (dashed arrow).

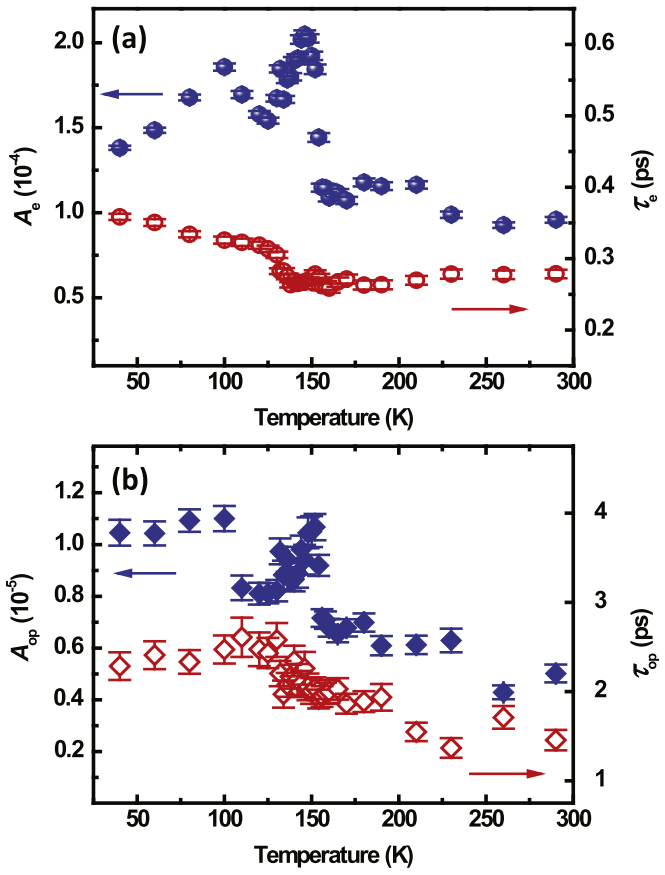

Figure 4. Temperature variations of the amplitude A_e and the decay time τ_e for the photoexcited electrons of $Sr_3Ir_4Sn_{13}$. (b) Temperature variations of the amplitude A_{op} and the decay time τ_{op} for the optical phonons of $Sr_3Ir_4Sn_{13}$.

arising from boson-mediated many-body interactions. Indeed, the enhancement of the effective mass in $Sr_3Ir_4Sn_{13}$ had been confirmed from the measurement of the optical conductivity at low temperatures [4]. Anomalous features previously noticed in the Hall and Seebeck coefficients near 100 K may be ascribed to the

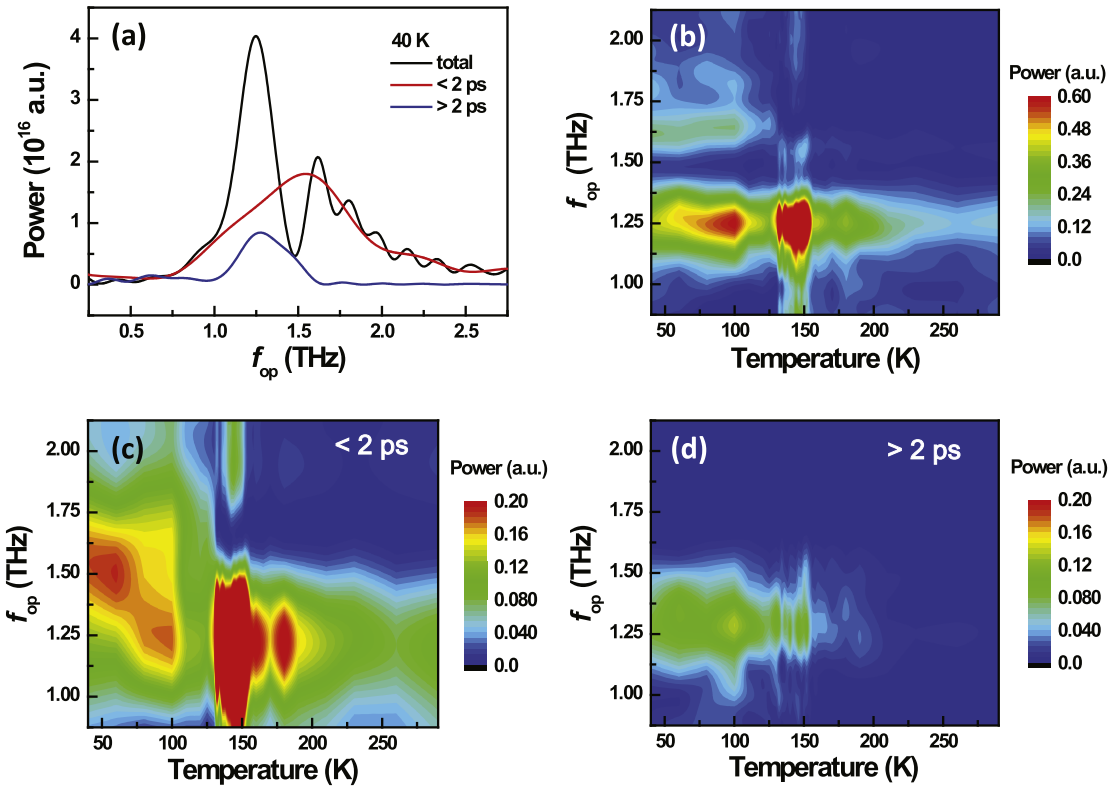

Figure 5. (a) The Fourier transform spectra obtained from the inset of figure 2(b). (b) The temperature-dependent Fourier transform spectra obtained from figure 1(a). (c) The temperature-dependent Fourier transform spectra obtained from figure 1(a) before 2 ps. (d) The temperature-dependent Fourier transform spectra obtained from figure 1(a) after 2 ps.

similar effects [3, 6], which may also cause the broad maxima A_{op} in figure 4(b) via the electron-phonon coupling.

As mentioned, the photoexcited electrons accumulated in the *d* conduction bands of $Sr_3Ir_4Sn_{13}$ quickly release their energy through the emission of optical phonons within several picoseconds. For each temperature, the dynamical behavior of the optical phonons associated with a fast oscillatory feature in $\Delta R/R$ can be described by a damped oscillatory function as $A_{op}e^{-t/\tau_{op}}\sin(2\pi f_{op}t + \phi_{op})$. Here A_{op} is related to the population of the optical phonons; τ_{op} is the corresponding damping time; f_{op} is the time-dependent oscillatory frequency; ϕ_{op} is the initial phase of the oscillation. The temperature variations of the resolved A_{op} and τ_{op} are given in figure 4(b). As one can see, the temperature dependences of A_{op} and τ_{op} are quite similar to the corresponding A_e and τ_e, exhibiting marked features near T^*. The strong similarity between photoexcited electrons and optical phonons gives evidence for their intimate correlation.

To explore the significant role of the probed phonons associated with the structural phase transition of $Sr_3Ir_4Sn_{13}$, we analyze the optical phonon energy, i.e, the oscillatory frequency f_{op} and illustrate its temperature variation in figure 5 through Fourier transform. There are two distinguishable modes in low-temperature region. However, only low-frequency mode of 1.25 THz (~5.2 meV) can be observed at $T > T^*$, which also shows a weak temperature dependence. It is noticeable that our data fail to indicate a characteristic of the phonon softening at around T^* as reported in the isostructural analogue of $Ca_3Ir_4Sn_{13}$ [16]. Indeed, a recent inelastic neutron scattering study of $Ca_3Ir_4Sn_{13}$ revealed a phonon softening feature at the excitation spectra where a phonon mode of 1.05 meV (~0.25 THz) has been found to shift towards lower energy on approaching its T^* of 38 K from high temperatures [16]. The observed soft phonon mode in $Ca_3Ir_4Sn_{13}$ has been assigned to the propagation wave-vector at $q = (1/2, 1/2, 0)$ predicated by the density functional theory (DFT) calculations as collaborating with its crystal structure [2, 16]. The indiscernible phonon softening behavior around the phase transition region of $Sr_3Ir_4Sn_{13}$ is likely due to the dominantly vibrational density of states at around 1.25 THz that overwhelms the contribution from the soft phonons with different energy.

In the low-T phase, an additional oscillatory mode of about 1.62 THz (~7.2 meV) has been identified. This phonon mode should arise from the larger phonon density of states associated with the corresponding phonon dispersion relations. In this regard, our observation provides a clear identification for a substantial change in the phonon dispersion undergoing the structural phase transition. It is remarkable that this mode exhibits softening behavior on approaching T^* from low temperatures, especially within 2 ps as shown in figure 5(c). This

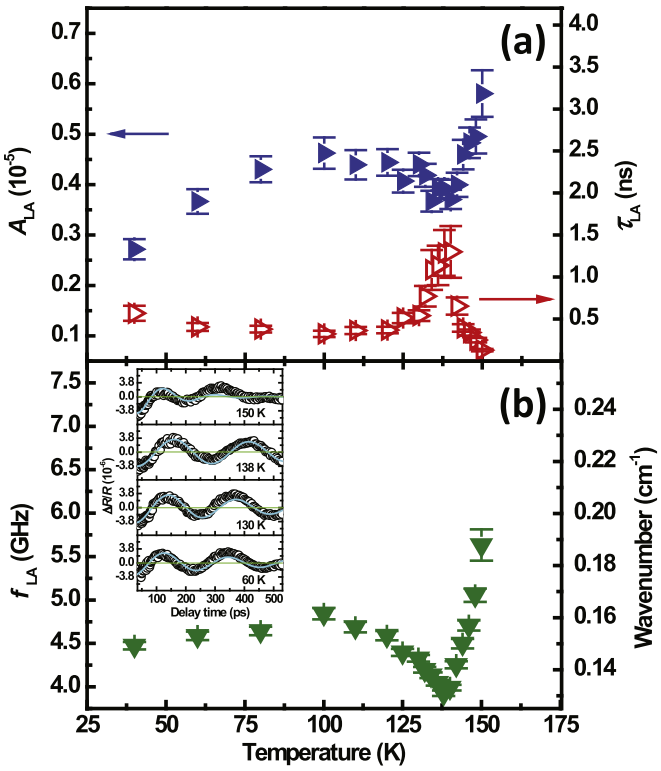

Figure 6. (a) Temperature variations of the amplitude A_{LA} and the decay time τ_{LA} for the GHz-range phonons of $Sr_3Ir_4Sn_{13}$. (b) Temperature dependence of the slow oscillatory frequency f_{LA}. The inset displays four representative oscillations taken at different temperature. Each associated solid curve is the damped sinusoidal fitting.

indicates that the high-frequency mode of 1.62 THz appears first after excitation by a pump pulse. After 2 ps, the high-frequency mode disappear and then the low-frequency mode of 1.25 THz come out due to the change of coupling constants for both modes or the energy transfer from 1.62-THz mode to 1.25-THz mode. The phonon softening feature bears a resemblance to the characters in the conventional CDW systems such as $K_{0.3}MoO_3$, 1*T*-TaS_2, and RTe_3 (R = Ho, Dy, Tb) revealed by time-resolved spectroscopy [17–20]. In those studies, the softening phenomena have been connected to the responses of the amplitude mode (AM) of the CDW. For example, the oscillation frequency of 1.7 THz in $K_{0.3}MoO_3$ shows clear softening as the critical temperature of 183 K is approached from below [17]. Since $Sr_3Ir_4Sn_{13}$ was proposed to be a new 3D superconductor with an unconventional CDW phase transition near 147 K, it is realistic that the modes observed at 1.62 THz and 1.25 THz in $Sr_3Ir_4Sn_{13}$ have a similar character as the amplitude modes seen in those low-dimensional CDW systems [17–20]. In other words, the 1.25-THz phonon in $Sr_3Ir_4Sn_{13}$ by symmetry would be coupled to the charge excitations of the charge-density wave. In the low-temperature I' phase structure [1], the movement of Sn coordinates in response to the phonon instabilities that dominates the low-energy mode. Consequently, the appearance of the 1.62-THz phonon can then be understood to arise from symmetry breaking below T^*.

In addition to the THz-range oscillatory behavior, we observed slow GHz-range oscillations in $\Delta R/R$ below 150 K, attributed to the dynamic response of the longitudinal-acoustic (LA) phonons caused by the interference between the probe beams reflected from the crystal surface and the rear interface of the propagating strain pulse with the modulated dielectric constant [21]. As in the case of high-frequency oscillations, each slow oscillation can be described by a damped oscillatory function as $A_{LA}e^{-t/\tau_{LA}}\sin(2\pi f_{LA}t + \phi_{LA})$. Here all parameters for the low-frequency phonons correspond to the same physical quantities as those for the optical phonons. In the inset of figure 6(b), we illustrate several representative oscillations with fitting curves. We thus extracted the $T-$ dependent A_{LA} and τ_{LA} for $Sr_3Ir_4Sn_{13}$ with results displayed in figure 6(a). It is apparent that both parameters exhibit dramatic changes in the vicinity of T^*, implying that the slow oscillatory phenomenon is also related to the structural phase transition. The $T-$ dependent f_{LA} is shown in figure 6(b), indicating a very pronounced softening feature around T^*. It is worthwhile mentioning that the LA phonon energy of about 0.087 meV (~21 GHz) in FeSe has been found to drop by 60% across its structural phase transition temperature around 90 K [22, 23]. With this respect, it seems reasonable to ascribe the slow oscillations in $Sr_3Ir_4Sn_{13}$ to the similar dynamics of the LA phonons. Additionally, the disappearance of LA phonons at high temperatures is possibly caused by the smaller penetration depth and larger refractive index [4] in the simple cubic parent structure (*I* phase) above T^*.

Recently, the GHz-range phonons have been detected from $\Delta R/R$ of $SrTiO_3$ and the softening across its phase transition at 105 K has been interpreted by the coupling of the phonons to the domain walls [24]. More specifically, the additional softening at 70 GHz has been argued to occur only when the strain wave amplitude is large enough for enhancing the coupling to the domain walls. It has been suggested that the domains may be formed along with the elongated axis in a particular direction within a crystal structure with low crystallographic symmetry [25]. For the present case of $Sr_3Ir_4Sn_{13}$, the single crystal XRD analysis has revealed a unit cell doubling below T^* driven by a subtle lattice distortion accompanied by lowering crystallographic symmetry [1]. Based on this, it would be qualitatively realistic to connect the observed softening of the GHz-range phonons to such a scenario.

3. Concluding remarks

We have investigated the ultrafast dynamics of the collective excitations in $Sr_3Ir_4Sn_{13}$ single crystals by dual-color femtosecond spectroscopy. Prominent features have been revealed near T^*, providing qualitatively new information about its structural phase transition. Two temporal oscillations in $\Delta R/R$ have been unambiguously resolved. The THz-range optical phonons exhibit a marked change across T^*, giving evidence for the modification of the phonon dispersion undergoing the structural phase transition. The GHz-range phonons which only appear below 150 K are thought to be the dynamic response of the longitudinal-acoustic phonons. It has been reported that the isostructural compounds $Ca_3Ir_4Sn_{13}$, $Sr_3Rh_4Sn_{13}$, $La_3Co_4Sn_{13}$, and $Ce_3Co_4Sn_{13}$ exhibit similar structural phase transitions [6, 16, 26–37]. Hence, it would be an interesting subject to clarify the possible uniformity of their structural phase transitions by utilizing the same ultrafast optical probe.

Acknowledgments

This work has been supported by the Ministry of Science and Technology of Taiwan under Grant Nos. MOST-103-2923-M-009-001-MY3, MOST-103-2628-M-009-002-MY3, MOST-103-2119-M-009-004-MY3 (CWL), MOST-103-2112-M-006-014-MY3 (CSL).

References

[1] Klintberg L E, Goh S K, Alireza P L, Saines P J, Tompsett D A, Logg P W, Yang J, Chen B, Yoshimura K and Grosche F M 2012 *Phys. Rev. Lett.* **109** 237008
[2] Tompsett D A 2014 *Phys. Rev.* B **89** 075117
[3] Kuo C N, Liu H F, Lue C S, Wang L M, Chen C C and Kuo Y K 2014 *Phys. Rev.* B **89** 094520
[4] Fang A F, Wang X B, Zheng P and Wang N L 2014 *Phys. Rev.* B **90** 035115
[5] Biswas P K, Amato A, Khasanov R, Luetkens H, Kefeng W, Petrovic C, Cook R M, Lees M R and Morenzoni E 2014 *Phys. Rev.* B **90** 144505
[6] Wang L M, Wang C-Y, Chen G-M, Kuo C N and Lue C S 2015 *New J. Phys.* **17** 033005
[7] Kamihara Y, Watanabe T, Hirano M and Hosono H 2008 *J. Am. Chem. Soc.* **130** 3296–7
[8] Rotter M, Tegel M and Johrendt D 2008 *Phys. Rev. Lett.* **101** 107006
[9] Paglione J and Greene R L 2010 *Nature Phys.* **6** 645
[10] Imai T, Ahilan K, Ning F L, McQueen T M and Cava R J 2009 *Phys. Rev. Lett.* **102** 107005
[11] de la Cruz C *et al* 2008 *Nature* **453** 899
[12] Dong J *et al* 2008 *Europhys. Lett.* **83** 27006
[13] Rotter M, Tegel M, Johrendt D, Schellenberg I, Hermes W and Pottgen R 2008 *Phys. Rev.* B **78** 020503
[14] Bao W *et al* 2009 *Phys. Rev. Lett.* **102** 247001
[15] Kase N, Hayamizu H and Akimitsu J 2011 *Phys. Rev.* B **83** 184509
[16] Mazzone D G *et al* 2015 *Phys. Rev.* B **92** 024101
[17] Demsar J, Biljakovic K and Mihailovic D 1999 *Phys. Rev. Lett.* **83** 800
[18] Demsar J, Forro L, Berger H and Mihailovic D 2002 *Phys. Rev.* B **66** 041101
[19] Yusupov R V, Mertelj T, Chu J-H, Fisher I R and Mihailovic D 2008 *Phys. Rev. Lett.* **101** 246402
[20] Yusupov R V, Mertelj T, Kabanov V V, Brazovskii S, Kusar P, Chu J-H, Fisher I R and Mihailovic D 2010 *Nature Phys.* **6** 681
[21] Thomsen C, Strait J, Vardeny Z, Maris H J, Tauc J and Hauser J J 1984 *Phys. Rev. Lett.* **53** 989
[22] Luo C W *et al* 2012 *Phys. Rev. Lett.* **108** 257006
[23] Luo C W *et al* 2012 *New J. Phys.* **14** 103053
[24] Maerten L, Bojahr A, Gohlke M, Rossle M and Bargheer M 2015 *Phys. Rev. Lett.* **114** 047401
[25] Carpenter M A 2007 *Am. Mineral.* **92** 309
[26] Yang J, Chen B, Michioka C and Yoshimura K 2010 *J. Phys. Soc. Jpn.* **79** 113705
[27] Wang K and Petrovic C 2012 *Phys. Rev.* B **86** 024522
[28] Gerber S, Gavilano J L, Medarde M, Pomjakushin V, Baines C, Pomjakushina E, Conder K and Kenzelmann M 2013 *Phys. Rev.* B **88** 104505
[29] Goh S K, Tompsett D A, Saines P J, Chang H C, Matsumoto T, Imai M, Yoshimura K and Grosche F M 2015 *Phys. Rev. Lett.* **114** 097002
[30] Kuo C N, Tseng C W, Wang C M, Wang C Y, Chen Y R, Wang L M, Lin C F, Wu K K, Kuo Y K and Lue C S 2015 *Phys. Rev.* B **91** 165141

[31] Liu H F, Kuo C N, Lue C S, Syu K-Z and Kuo Y K 2013 *Phys. Rev.* B **88** 115113
[32] Slebarski A, Fijalkowski M, Maska M M, Mierzejewski M, White B D and Maple M B 2014 *Phys. Rev.* B **89** 125111
[33] Thomas E L, Lee H O, Bankston A N, MaQuilon S, Klavins P, Moldovan M, Young D P, Fisk Z and Chan J Y 2006 *J. Solid State Chem.* **179** 1642
[34] Lue C S, Liu H F, Hsu S L, Chu M W, Liao H Y and Kuo Y K 2012 *Phys. Rev.* B **85** 205120
[35] Slebarski A and Goraus J 2013 *Phys. Rev.* B **88** 155122
[36] Slebarski A, Goraus J and Witas P 2015 *Phys. Rev.* B **92** 155136
[37] Lue C S, Kuo C N, Tseng C W, Wu K K, Liang Y H, Du C H and Kuo Y K 2016 *Phys. Rev.* B **93** 245119